ELSEVIER

Multiple scattering of light in a resonant medium

G. Labeyrie [a], D. Delande [c], C.A. Müller [b], C. Miniatura [a], R. Kaiser [a,*]

[a] *Institut Non Linéaire de Nice, UMR 6618 CNRS, 1361 route des Lucioles, F-06560 Valbonne, France*
[b] *Universität Bayreuth, D-95440 Bayreuth, Germany*
[c] *Laboratoire Kastler Brossel, Université Pierre et Marie Curie, 4 Place Jussieu, F-75005 Paris, France*

Abstract

We investigate some signatures of multiple scattering of light in a vapor of laser-cooled rubidium atoms. This sample presents several unusual properties when compared to classical samples i.e. white paper or suspensions of dielectric particles: a very strong resonance, an internal structure of the atomic scatterer, and a spherically symmetric geometry with a quasi-Gaussian density profile. We study how the light frequency modifies static quantities such as the coherent transmission, the diffuse transmission and reflection, and the coherent backscattering cone. The experimental data are compared to a Monte Carlo simulation including all experimental parameters.
© 2004 Elsevier B.V. All rights reserved.

The propagation of waves in random scattering media, a field which originated in astrophysics at the beginning of the last century [1], has received a renewed interest since the 1980s. Apart from various potential applications e.g. in medical imaging, a more fundamental reason for this interest lies in the role played by interferences. Indeed, it was realized that interference between scattered waves can affect the transport in such media [2], emphasizing the need for theories going beyond the radiative transfer treatment [3]. Many manifestations of such phenomena have been reported in optics including coherent backscattering (CBS) [4], universal conductance fluctuations [5] and strong localization [6]. Among many kinds of media used so far in studies of coherent multiple scattering of light, cold atomic gases have recently appeared [7,8]. These samples have some very unusual properties, which allow to study new regimes or new physical situations [7,9–11]. They also constitute a new tool to validate fundamental theories of

---
[*] Corresponding author. Tel.: +33 1 92 96 73 91; fax: +33 1 93 65 25 17.
E-mail addresses: Guillaume.Labeyrie@inln.cnrs.fr (G. Labeyrie), Robin.Kaiser@inln.cnrs.fr (R. Kaiser).

light transport [12,13]. One striking property of the atomic scatterer is the presence of extremely narrow resonances (quality factor $Q \simeq 10^8$). The advent of laser-cooling techniques has allowed to produce collections of atoms with a negligible Doppler broadening, which thus constitutes a *monodisperse* sample of highly resonant scatterers. As a consequence, the light mean-free path in such samples can be varied over orders of magnitude by simply tuning the light frequency a few MHz away from the resonance. We illustrate this aspect in the present paper, by measuring the frequency response of various quantities linked to multiple scattering.

We present some measurements of the coherent transmission, diffuse reflection and transmission, and CBS signal as a function of the laser detuning from the atomic resonance. We compare these data with Monte Carlo (MC) simulations including all the experimental parameters, such as the sample geometry and the complex atomic internal structure.

In the present experiments, we use a probe light quasi-resonant with the $F = 3 \rightarrow F' = 4$ transition of the D2 line of Rb^{85} (wavelength $\lambda = 780$ nm, linewidth $\Gamma/2\pi = 5.9$ MHz). This atomic system is quite far from an ideal 2-level system. First, the ground state $F = 3$ consists of seven degenerate Zeeman-sublevels. We will assume in the following that the atoms in the cloud are evenly distributed among these sublevels, and neglect optical pumping. Second, there are two other excited states accessible in the hyperfine structure multiplet, namely the $F' = 3$ and $F' = 2$ levels which are distant from the $F' = 4$ state by 20 and 30 natural widths, respectively. Although we will remain tuned within four natural widths from the $F' = 4$ level, we will see that the influence of these far-detuned transitions can in principle be detected [14]. The experimental setup to produce the optically thick cloud of cold atoms and record the CBS signal has already been described [7]. We just recall here the typical parameters characterizing our sample of cold atoms, obtained from a vapor-loaded magneto-optical trap (MOT). It consists of a cloud with a roughly Gaussian density profile of average rms radius $r_0 = 2$ mm typically (the cloud shape is usually anisotropic). The rms velocity (modulus) is 0.1 m/s (temperature in the 100 μK range). Thus, the residual Doppler broadening is much smaller than the width of the resonance ($kv_{\text{rms}}/\Gamma \simeq 1/30$) and the sample can be considered monodisperse [15]. The optical thickness along a diameter is defined by $b = -ln(T_c) = \sqrt{2\pi}r_0/\ell$ where ℓ is the *minimum* light mean-free path at the center of the cloud, and T_c the coherent transmission coefficient. Since the atomic scatterers are resonant, both quantities depend strongly on the detuning from resonance $\delta = \omega - \omega_0$ (ω and ω_0 being the light and atomic transition angular frequencies, respectively). The minimum mean-free path is given by $\ell = 1/(\sigma n)$ where σ is the total scattering cross-section and n the atomic density at the center of the cloud. If we neglect the off-resonant transitions, the cross-section writes

$$\sigma = g\frac{3\lambda^2}{2\pi}\frac{1}{1 + (2\delta/\Gamma)^2}, \tag{1}$$

where $g = 3/7$ is the degeneracy factor of the transition. Thus, the light mean-free path increases quadratically with the detuning from resonance and can be varied by orders of magnitude by simply tuning the light frequency by a few natural widths. Accordingly, the optical thickness varies as a Lorentzian with detuning:

$$b(\delta) = \frac{b_0}{1 + (2\delta/\Gamma)^2}, \tag{2}$$

where b_0 is the optical thickness at resonance. The maximum value obtained with the present setup is about 40, which corresponds to a peak density $n \simeq 6 \times 10^{10}$ cm^{-3} and a total number of atoms in the cloud of almost 10^{10}. The mean-free path at cloud center is then $\ell \approx 120$ μm, which means that we operate in the dilute regime $k\ell \approx 1000 \gg 1$. Fig. 1 shows a schematic view of the arrangement used to measure the various quantities. In order to record the CBS cone, a laser beam of uniform intensity and diameter 9 mm (i.e. larger than the cloud) is employed. The angular distribution of the backscattered light is recorded, after selection of the polarization, on a CCD placed in the focal plane of a lens. The CBS peak is obtained after averaging the backscattered intensity over many sample configurations (i.e.
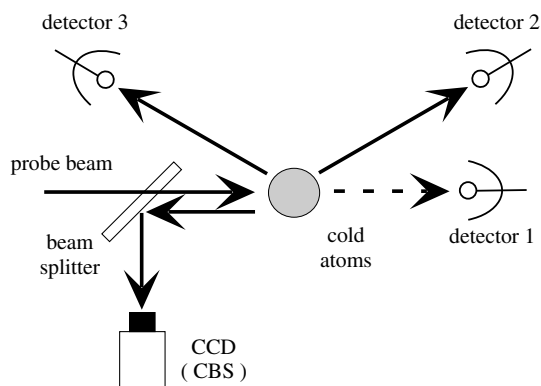
Fig. 1. Geometry for the detection of multiple scattering signals. We measure the coherent transmission T_c (detector 1), the diffuse transmission T_d (detector 2) and reflection R_d (detector 3), and the coherent backscattering signal (CBS).

Fig. 2. Coherent transmission T_c. We plot the measured coherent transmission (circles) as a function of the detuning from resonance, expressed in units of the natural width Γ. We extract from the width of this curve the optical thickness on resonance $b_0 \simeq 35$. The solid line is the theoretical transmission assuming a Lorentzian spectrum of FWHM = 2 MHz for the laser.

respective positions of the atoms in the cloud). To measure the reflected and transmitted intensities, we send a laser beam of diameter 2 mm through the center of the cloud. The diffuse reflection R_d and transmission T_d are both detected at an average angle of about $20°$ from the incident beam direction. The solid angle of collection of the scattered light is 0.02 srd for both measurements. All measurements (including CBS) are performed with the same probe intensity, resulting in a saturation parameter at resonance $s_0 = 0.05$, and the same probe duration of 200 μs. Thus, the maximum number of photons scattered by one atom is approximately 180. Since the probability for hyperfine pumping at $\delta = 0$ is of the order of 10^{-3}, this process should remain quite small in the vicinity of the $F = 3 \rightarrow F' = 4$ transition.

Fig. 2 shows the coherent transmission curve recorded by varying the detuning around resonance. For each detuning value, the transmitted intensity (in the presence of cold atoms) is divided by the incident intensity (no cold atoms) to yield the coherent transmission T_c. The large on-resonance optical thickness is responsible for the flat transmission in a wide frequency range around resonance. The non-zero transmission in this range is due to the finite linewidth of our probe laser (about 2 MHz): for a resonant excitation ($\delta = 0$), the detected intensity is the integral over the whole spectrum of the product of the laser spectrum by the
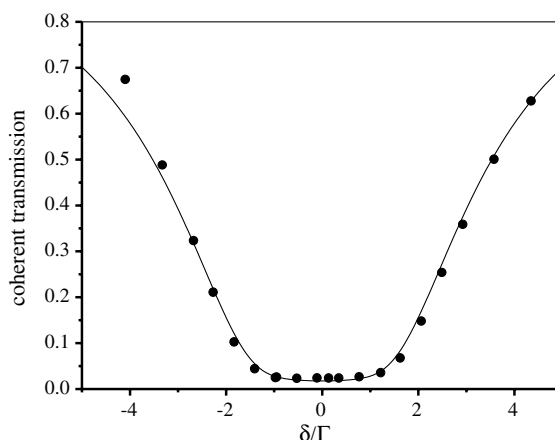
monochromatic transmission, which can be very crudely approximated by a rectangular notch filter of spectral width Δv. If the wings of the laser spectrum contain enough power outside of this range, the on-resonance transmission will be much larger than e^{-b_0} [16]. For a Lorentzian spectrum, this is true even if the laser linewidth is much smaller than Γ. Thus, we extract the on-resonance optical thickness from the FWHM Δv of the coherent transmission curve. Indeed, for high enough optical thicknesses (such as $T_c \ll 1$) one has $\Delta v \approx \Gamma \times \sqrt{(b/ln2 - 1)}$. The width Δv is then a much more reliable parameter to estimate the optical thickness than the direct transmission at $\delta = 0$ (at least for large optical thicknesses). We obtained from the data in Fig. 2 a width $\Delta v = 7\Gamma$, yielding $b_0 \simeq 35$. The cloud shape is anisotropic with rms radii $r_x = 1.9$ mm, $r_y = 3.0$ mm and $r_z = 2.0$ mm (x and y are orthogonal to the incident wave vector). Note the small asymmetry of the measured transmission in Fig. 2: the transmission is slightly higher for negative than for positive detunings. We believe this could originate either from hyperfine pumping to the $F = 2$ ground state, which is more likely on the red side and reduces the probed optical thickness, or by mechanically pushing the

atoms out of resonance. Fig. 3 shows both the diffuse reflected (stars) and transmitted (squares) intensities as a function of the light detuning. Their respective maxima have been scaled to unity to ease the comparison. The coherent transmission curve of Fig. 2 is also reproduced here. One observes for the diffuse reflection a broad, quasi-Lorentzian curve of FWHM = 4.2Γ (see discussion below). On the contrary, the diffuse transmission exhibits a double-peaked behavior resulting from a minimum transmission at $\delta = 0$ and maxima around $\delta \simeq \pm 2.4\Gamma$. One expects the total number of photons to be conserved (i.e. all the photons leaving the probe should contribute to the diffuse intensity), thus it is not surprising that a minimum diffuse transmission corresponds to a maximum diffuse reflection. However, to verify the conservation of the total number of photons would require integrating the diffuse intensity over the whole 4π solid angle. To understand qualitatively the curves of Fig. 3, let us re-plot these data in Fig. 4 but this time as a function of the optical thickness $b(\delta)$ (positive detunings only). To simplify the discussion, we consider a transversely infinite slab whose optical thickness is gradually increased. At small optical thickness $b \ll 1$, we are in the single scattering regime. If the radiation pattern of the scatterers is
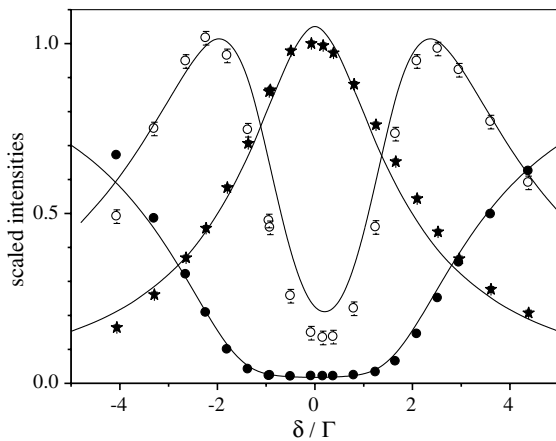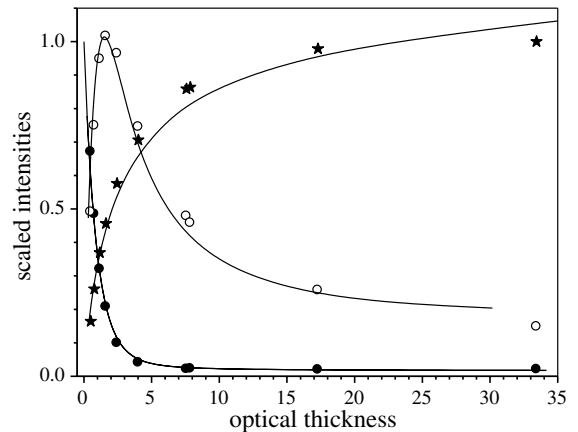

Fig. 4. Normalized diffuse reflection and transmission, and coherent transmission as a function of optical thickness. Same data as in Fig. 3, this time plotted as a function of the optical thickness $b(\delta)$ ($\delta > 0$ only). The solid lines are the MC results.

Fig. 3. Normalized diffuse reflection R_{d} and transmission T_{d} as a function of laser detuning. We measured the diffuse reflected (stars) and transmitted (squares) intensities, as a function of the detuning from resonance. The coherent transmission of Fig. 2 is also plotted for comparison (circles). The solid lines are the results of the MC simulations.

symmetric with respect to the transverse plane, both diffuse transmission and reflection are equal and small, since most of the light passes through the sample without being scattered. Thus, when b increases both quantities increase by the same amount. The reflection increases in a monotonous way up to unity: in the limit of a semi-infinite medium all the light is reflected. On the other hand, the diffuse transmission obviously admits a maximum since it should decrease toward zero for large b. Numerical calculations in the case of an homogenous slab show that this maximum occurs for $b = 2$ [19]. We see that the curves of Fig. 4 closely match the behavior discussed above. Considering for instance the diffuse transmission, one observes a low value at large optical thickness b (i.e. for $\delta \simeq 0$ in Fig. 3), which then increases as b decreases (i.e. as $|\delta|$ increases) and reaches a maximum around $b = 1.6$. This critical value determines the position of the maxima in Fig. 3, which occur at δ such as $b(\delta) = 1.6$. Note that for low optical thickness $b_0 < 1.6$ the double peak structure is replaced by a bell-shaped curve which approaches a Lorentzian of width Γ in the single scattering limit ($b_0 \ll 1$). Using the results of [19], one can approximate the diffuse reflection by $\eta b/(1 + \eta b)$, where η is a constant $\simeq 0.4$. Since $b(\delta)$ is a Lorentzian, it is straightforward to show that $R_{\mathrm{d}}(\delta)$ is also a Lorentzian, of width $\sqrt{1 + \eta b_0}\,\Gamma$ (see Fig. 3). The

discussion above shows that, for these multiple scattering quantities, the only relevant parameter is the optical thickness which is itself determined by a combination of several parameters: total number of atoms and size of the cold cloud, and laser detuning. The curves on Fig. 4 could also be obtained e.g. at fixed detuning by varying the number of atoms in the MOT.

Our sample geometry is more complex than a uniform slab as will be further emphasized later. In particular, it is the finite transverse extension that motivates the use of a beam much smaller than the cloud size (a larger beam would wash out the "double-bump" signature). To analyze quantitatively these data, we use the MC simulation described in [20]. The simulation includes all experimental parameters such as cloud and detection geometry, laser spectrum and atomic residual velocity [21]. There is no adjustable parameter. However, by looking closely at Fig. 3 one can notice a small shift (of about 0.2Γ) of the diffuse transmission curve. The corresponding MC curve was shifted by the same amount. The MC results correspond to the solid curves in Figs. 3 and 4. As can be seen, the overall agreement is quite satisfactory. The quantities discussed so far present no signature of interference effect in multiple scattering, and can be analyzed using the radiative transfer theory. We now turn to the most accessible signature of such interferential corrections: the CBS effect. The CBS interference results in an enhancement of the configuration-averaged reflected intensity in a narrow angular range of width $\Delta\theta$ around exact backscattering (see Fig. 5). This enhancement, defined as the ratio of the peak value ($\theta = 0$) to the background value ($\theta \gg \Delta\theta$), is equal to 2 for classical samples if the proper polarization configuration is selected [4]. The results presented in this paper correspond to CBS peaks recorded in the so-called orthogonal helicity channel (circular incident polarization, detection of opposite helicity), which yields the highest enhancement for rubidium [22], as a function of the laser detuning. Before any analysis, the raw CBS images are angularly averaged to improve the signal-to-noise ratio. Fig. 5 shows an example of such a CBS peak, obtained for $\delta \approx \Gamma$. The peak value (here $\simeq 1.15$) is much smaller than
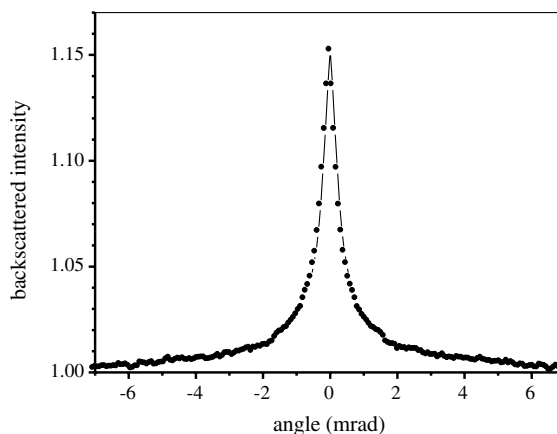

Fig. 5. Example of CBS peak: experimental result (circles) and Monte Carlo simulation (line). This signal is recorded in the orthogonal helicity channel, for $\delta \approx \Gamma$.

2 because of the degeneracy in the ground state of the Rb atom [22]. We now discuss the behavior of the CBS cone angular width $\Delta\theta(\delta)$, which is plotted in the inset in Fig. 6 (symbols: experiment, line: MC). The measured CBS peaks are significantly broader ($\approx 20\%$ on average) than the simulated ones. This discrepancy could originate in the detailed shape of the longitudinal density profile around unit optical depth, which has a strong
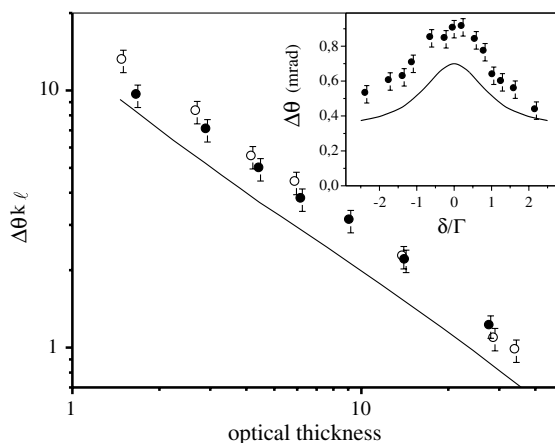

Fig. 6. Width of the CBS cone (symbols: experiment, line: Monte Carlo simulation). We plot here the reduced width $\Delta\theta k\ell$ of the CBS peak as a function of the optical thickness. The solid and open circles correspond, respectively, to blue ($\delta > 0$) and red ($\delta < 0$) detunings. Note the double logarithmic scale. The inset shows the corresponding variation of the cone width $\Delta\theta$ as a function of δ.

influence on the CBS width [20]. A striking feature of Fig. 6 is the overall small variation of the cone width as the detuning is increased (less than a factor 2). Indeed, in a homogenous medium the cone width is inversely proportional to the mean-free path. In the present experiment, the mean-free path varies by more than a factor 20! We have shown in [20] that this surprising behavior originates from the non-uniform *longitudinal* density profile of the sample. Qualitatively, the cone width is determined by the local mean-free path *at unit optical depth* which is roughly *constant* with detuning (as long as the optical thickness remains $\gg 1$) and of the order of the sample size. We also show in Fig. 6 how the reduced CBS width $\Delta\theta k\ell$ varies with the optical thickness. The solid and open symbols correspond to positive and negative light detunings, respectively. The distinctive linear dependence in log–log scale is a signature of the ''bell-shaped'' longitudinal density profile of our sample (in a homogenous slab, $\Delta\theta k\ell$ would saturate at ≈ 0.7 for high optical thicknesses) [20]. Let us now turn to the analysis of the CBS enhancement factor, whose variation is reported in Fig. 7 as a function of the optical thickness (solid and open circles correspond to $\delta > 0$ and < 0,

respectively). The solid line is the result of the MC simulation. The CBS peak heights measured in this experiment are slightly lower than the theoretical prediction (by $\approx 10\%$). This could be due to e.g. a non-uniform distribution of the atoms in the Zeeman ground states. The MC curves in Figs. 7 and 8 have been rescaled accordingly for a better comparison with the experimental data. As emphasized above, the internal degeneracy of an atomic ground state with angular momentum $F > 0$ is responsible for the small observed enhancement factor in all polarization channels. Its precise value is determined by the relative amount of single scattering versus the multiple scattering interference contrast and thus depends on the optical thickness of the sample (whereas for classical samples with perfect interference, the enhancement factor is 2 in the parallel helicity channel regardless of the optical thickness). The interference contrast decreases exponentially with the scattering order or path length, such that samples with large optical thickness show a small overall enhancement. On the other hand, for very small optical thickness, single scattering dominates, and the enhancement is also very small. Between these two extremes, a maximum enhancement is found
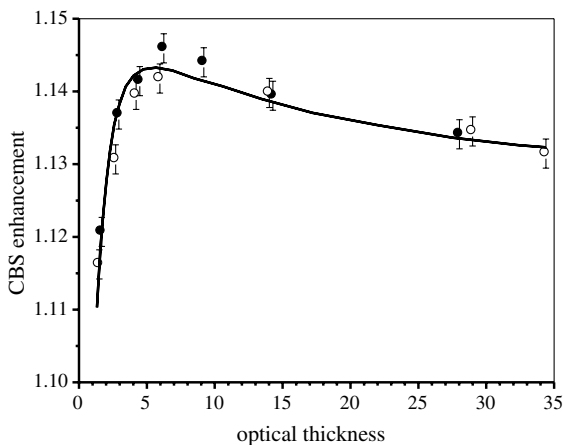

Fig. 7. CBS enhancement factor as a function of optical thickness. We report here the CBS enhancement factor α (orthogonal helicity channel) as a function of the optical thickness b of the cloud. The solid and open circles correspond to a blue- and re-detuned laser, respectively. The line is the MC result (see text).
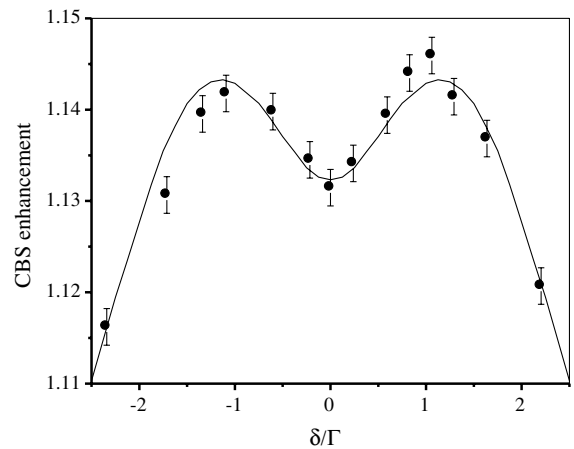

Fig. 8. Asymmetry of the CBS enhancement. We plot this time the CBS enhancement as a function of the laser detuning. The general features (dip around $\delta = 0$, maximum around $\delta = 1$) arise from the atomic internal structure, as in Fig. 7. Note the small asymmetry between the red- and blue-detuning domains (see discussion in text). The solid line is a MC simulation.

at an optical thickness with minimum single scattering and maximum multiple scattering contrast. In our case, this optimum is reached for $b \approx 6$ [22] as can be seen in Fig. 7. For smaller detunings (i.e. larger optical thicknesses), the enhancement decreases because of an increasing relative weight of high scattering orders $N > 2$ which contribute little to the interference. For larger detunings (i.e. smaller b's) the enhancement decreases because of the increasing amount of single scattering. We now plot in Fig. 8 the variation of the enhancement as a function of laser detuning. The ''double bumped'' behavior is a manifestation of the internal structure as discussed previously, the maxima around $|\delta| \approx \Gamma$ corresponding to the critical optical thickness of 6. Note the small blue–red *asymmetry* of the measured enhancement factors. Such an asymmetry has been predicted by Kupriyanov et al. [14] as arising from the contributions of the other (far detuned) transitions accessible from the ground level $F = 3$. This has two consequences: first, the differential atomic cross-section for elastic scattering now contains interferential corrections depending on the detuning value; second, optical hyperfine pumping can occur which is accompanied by the emission of a photon detuned by 3 GHz (inelastic scattering). This photon sees a transparent medium and leaves the cloud. We are currently working on the inclusion of these effects in our theoretical treatment. The sign and order of magnitude of the observed effect seem compatible with what is theoretically predicted in [14]. However, we also observed that this small asymmetry is very sensitive to the specific experimental conditions, and in particular to the compensation of the magnetic field at the center of the MOT. A more careful study is thus necessary to detect unambiguously the effect of the far-off resonant transitions.

In conclusion, we have reported in this paper an experimental study of multiple scattering of light in a highly resonant cloud of cold rubidium atoms. Our results are in good agreement with existing theories of multiple scattering, with the additional inclusion of the atomic internal structure. The only relevant parameter for most of our data is the optical thickness of the sample. In contrast with previous multiple scattering experiments, the light mean-free path can here be *continuously* adjusted without manipulation of the sample. These results illustrate the new regimes that can be reached using cold gases to study mesoscopic physics.

References

[1] A. Schuster, Astrophys. J. 21 (1905) 1.
[2] E. Akkermans, G. Montambaux, J.-L. Pichard, J. Zinn-Justin, Mesoscopic Quantum Physics, Elsevier Science B.V., North-Holland, Amsterdam, 1995.
[3] S. Chandrasekhar, Radiative Transfer, Dover, New York, 1960.
[4] B.A. van Tiggelen, A. Lagendijk, A. Tip, J. Phys. Condens. Matter 2 (1992);
D.S. Wiersma, M.P. van Albada, B.A. van Tiggelen, A. Lagendijk, Phys. Rev. Lett. 74 (1995) 4193.
[5] F. Scheffold, G. Maret, Phys. Rev. Lett. 81 (1998) 5800.
[6] D. Wiersma, P. Bartolini, A. Lagendijk, R. Righini, Nature 390 (1997) 671.
[7] G. Labeyrie, F. de Tomasi, J.-C. Bernard, C.A. Müller, C. Miniatura, R. Kaiser, Phys. Rev. Lett. 83 (1999) 5266.
[8] P. Kulatunga, C.I. Sukenik, S. Balik, M.D. Havey, D.V. Kupriyanov, I.M. Sokolov, Phys. Rev. A 68 (2003) 033816.
[9] G. Labeyrie, C. Miniatura, C.A. Müller, O. Sigwarth, D. Delande, R. Kaiser, Phys. Rev. Lett. 89 (2002) 163901.
[10] O. Sigwarth, G. Labeyrie, T. Jonckheere, D. Delande, R. Kaiser, C. Miniatura, Phys. Rev. Lett. 93 (2004) 143906.
[11] Thierry Chanelière, David Wilkowski, Yannick Bidel, Robin Kaiser, Christian Miniatura, Phys. Rev. E 70 (2004) 036602.
[12] G. Labeyrie, E. Vaujour, C.A. Müller, D. Delande, C. Miniatura, D. Wilkowski, R. Kaiser, Phys. Rev. Lett. 91 (2003) 223904.
[13] A. Lagendijk, B.A. van Tiggelen, Phys. Rep. 270 (1996) 143;
M.C.W. van Rossum, T.M. Nieuwenhuizen, Rev. Mod. Phys. 70 (1999) 313.
[14] D.V. Kupriyanov, I.M. Sokolov, P. Kulatunga, C.I. Sukenik, M.D. Havey, Phys. Rev. A 67 (2003) 013814.

[15] Note, however, that for a high number of scattering events the light frequency accumulates a Doppler shift that cannot be neglected [12].

[16] This polychromatic effect is also responsible for a non linear behavior of the Faraday rotation at high optical thickness [17,18].

[17] G. Labeyrie, C. Miniatura, R. Kaiser, Phys. Rev. A 64 (2001) 033402.

[18] G.S. Agarwal, S. Dasgupta, Phys. Rev. A 67 (2003) 063802.

[19] H.C. van de HulstMultiple Light Scattering, vol. 2, Academic Press, London, 1980.

[20] G. Labeyrie, D. Delande, C.A. Müller, C. Miniatura, Robin Kaiser, Phys. Rev. A 67 (2003) 033814.

[21] The residual velocity spread is accounted for in the computation of the diffuse intensity, but not in the CBS simulation. The role of the temperature, quite negligible in this paper, is the subject of a publication in preparation.

[22] G. Labeyrie, D. Delande, C.A. Müller, C. Miniatura, Robin Kaiser, Europhys. Lett. 61 (2003) 327.